Research in Veterinary Science 129 (2020) 59–65

Contents lists available at ScienceDirect

Research in Veterinary Science

journal homepage: www.elsevier.com/locate/rvsc

Correlation between renal histopathology and renal ultrasound in dogs

Silvia Burti[a], Alessandro Zotti[a], Federico Bonsembiante[a,b], Giorgia Mastellaro[a], Tommaso Banzato[a,*]

[a] Department of Animal Medicine, Production and Health, University of Padua, Viale dell'Università 16, Agripolis, Legnaro, 35020, Padua, Italy
[b] Department of Comparative Biomedicine and Food Science, University of Padua, Viale dell'Università 16, Agripolis, Legnaro, 35020 Padua, Italy

ARTICLE INFO

Keywords:
Kidney
Ultrasound
Pathology

ABSTRACT

Fifty-three privately owned dogs were included in the study. Ultrasonography of the kidneys was performed *ante mortem*. All the dogs died or were euthanized for reasons unrelated to this study. Histopathology of both kidneys was performed, and a degeneration and an inflammation score ranging from zero to two was assigned by consensus between two pathologists. A numerical score based on a three level semi-quantitative scale (0, 0.5, 1) was assigned by consensus between two of the authors to the following ultrasonographic abnormalities: cortico-medullary definition, echogenicity of the renal cortex, echogenicity of the medulla, renal shape, cysts, scars, mineralizations, subcapsular perirenal fluid accumulation, pyelectasia. The scores deriving from the consensus were summed to create a summary index called renal ultrasound score (RUS). Statistically significant differences in cortico-medullary definition, echogenicity of the renal cortex, echogenicity of the medulla, renal shape, scars and pyelectasia were evident between the degeneration score groups. There were significantly different distributions of cortico-medullary definition, renal shape and scars between the inflammatory score groups. There were statistically significant differences in the RUS between the degenerative score groups ($F = 24.154$, p-value $< .001$). Post-hoc tests revealed significant differences between all groups. There were no significant differences in the RUS between the inflammatory score groups ($F = 1.312$, p-value $= .264$). Post-hoc tests revealed no significant differences between groups. The results of the present study suggest that the number and severity of the ultrasonographic abnormalities are correlated with the severity of the kidney degeneration. On the other hand, inflammation showed poor influence on the ultrasonographic appearance of the kidneys.

1. Background

B-mode ultrasonography (US) is commonly performed as part of the routine clinical evaluation of dogs with confirmed or suspected renal pathology (Bragato et al., 2017; Espada et al., 2006; Ivancic and Mai, 2008; Mattei et al., 2019; Morrow et al., 1996; Wang et al., 2013). Despite the widespread use of US, the correlation between ultrasound features and the actual histopathological condition of renal tissues, along with the diagnosis and follow-up of canine chronic kidney disease, is still debated (Bragato et al., 2017). The normal US appearance of the kidneys in dogs, taking into account individual variability, has been described in detail (Manley and O'Neill, 2001; Ivancic and Mai, 2008; Hart et al., 2013), and some studies investigating the relationship between renal function and renal ultrasound have been published in the last two decades (Espada et al., 2006; Lee et al., 2017; Mattei et al., 2019; Moghazi et al., 2005; Morrow et al., 1996). The relationship between renal cortical echogenicity and renal pathology has been investigated both *ex-vivo* (Manley and O'Neill, 2001) and *in-vivo* (Mattei et al., 2019; O'Neill, 2000) but, to the best of the authors' knowledge, a systematic comparison between renal ultrasound abnormalities and renal histopathology is still absent in veterinary literature.

The aim of this study is to evaluate the relationship between individual renal ultrasonographic abnormalities and both renal degeneration and inflammation as determined by histopathology. Furthermore, a new descriptive parameter, based on the sum of the US abnormalities, to objectively describe the relationship reported above is proposed.

2. Methods

2.1. Animals

All the animals included in this study were admitted for clinical consultation at the Veterinary Teaching Hospital, University of Padua, Italy, from January 2015 to March 2019. Ultrasound was part of the routine clinical evaluation and was performed within 24 h prior to

* Corresponding author.
E-mail address: tommaso.banzato@unipd.it (T. Banzato).

https://doi.org/10.1016/j.rvsc.2020.01.003
Received 17 July 2019; Received in revised form 23 December 2019; Accepted 2 January 2020

death.

All the animals died or were euthanized due to critical medical conditions unrelated to the purposes of this study. The cadavers were donated to the University Veterinary Hospital of the University of Padua by the owners. A full post-mortem examination was performed within 3 h of death and both kidneys were collected and fixed in 4% buffered formalin. Three transverse sections at the level of the cranial pole, the caudal pole and the renal hilum were sampled, in order to have an overview of the condition of each kidney. All the procedures were carried out respecting the relevant Italian and EU legislation concerning Animal Protection and Welfare (Leg. Decree 26/2014 implementing the EU directive 2010/63/EU). Since the data used in this study was collected as part of routine clinical activity, no ethical committee approval was needed. Informed consent regarding personal data processing was obtained from the owners.

2.2. Ultrasonography procedures

All the B-mode ultrasonographic examinations were performed by one of the authors of this study (TB, with over 9 years of experience in small animals' ultrasonography). The images were acquired with two different micro-convex probes (4–9 MHz and 5–8 MHz) connected to two ultrasonographic scanners: Zonare, Zonare Medical Systems Inc., Mountain View, California, USA, and Philips Affiniti 50, Italy – respectively. The images were then stored as digital imaging and communications in medicine (DICOM) files. Each kidney was scanned in a transverse and a longitudinal plane. Gain and time-gain compensation were manually adjusted to optimize image quality.

2.3. Image analysis procedures

All the DICOM images were reviewed independently by two of the authors, TB and AZ, with over 9 and over 19 years' experience in small-animal ultrasound respectively. The grading was concorded between the two authors following a consensus discussion; more specifically, after completion of the individual grading, consensus between the two evaluators was used to decide the final grade. The following renal abnormalities were recorded: 1) cortico-medullary definition, 2) echogenicity of the renal cortex, 3) echogenicity of the medulla, 4) renal shape, 5) cysts, 6) scars, 7) mineralizations, 8) subcapsular perirenal fluid accumulation, 9) pyelectasia. A numerical score based on a three-level qualitative scale (0, 0.5, 1) was assigned to each abnormality based both on its presence or absence and on its characteristics, as follows: cortico-medullary definition was classified as normal (0), slightly decreased (0.5), markedly decreased (1); echogenicity of the cortex and of the medulla was classified as normal (0), increased (0.5), heterogenous (1); renal shape was evaluated as normal (0), irregular (0.5), asymmetrical (1); the presence of cysts, scars and mineralizations was evaluated as absent (0), one (0.5), multiple (1); perirenal fluid and pyelectasia were graded as absent (0), slight (0.5) marked (1). Lastly, the scores deriving from the consensus were summed to create a summary index named renal ultrasonographic score (RUS).

2.4. Histopathological analysis

Histological analyses were performed on formalin-fixed, paraffin-embedded kidney samples. Three-μm histological slides were obtained from the three sampled portions of both right and left kidney. The slides were stained with haematoxylin and eosin, periodic acid-Schiff (PAS) and Masson's trichrome stains. Each kidney was considered as an independent sample. Classification of the morphological lesions was defined *a priori* and included: 1) glomerulosclerosis, 2) glomerulonephritis, 3) glomerular atrophy, 4) glomerular lipidosis, 5) tubular vacuolar degeneration, 6) interstitial nephritis, 7) tubular atrophy, 8) tubular necrosis, 9) fibrosis, 10) amyloidosis, 11) neoplasia. All the histopathological lesions were recorded as present or absent and reported as a dichotomous variable. Moreover, a 0-to-2 (0 = none, 1 = moderate, 2 = severe) semi-quantitative degenerative (including glomerulosclerosis, glomerular atrophy, glomerular lipidosis, tubular vacuolar degeneration, tubular atrophy, tubular necrosis, fibrosis and amyloidosis) and inflammatory (including glomerulonephritis and interstitial nephritis) grading system, modified from previously published papers (Aresu et al., 2013; Cianciolo et al., 2016), were applied to each sample. In particular: Glomerulosclerosis was graded as severe when the increase in the mesangial matrix (segmental to global) was evident in most glomeruli (> 50%) and many capillary loops appeared obliterated; moderate if the increase in the mesangial matrix was less severe. Glomerulonephritis was defined as severe if the hypercellularity (segmental to global) was evident in most glomeruli (> 50%); moderate if the hypercellularity involved < 50% of the glomeruli. Glomerular atrophy was defined as severe if > 50% of the glomeruli was classified as atrophic (small glomerular remnants composed of residual matrix and few cells); moderate when only 10% to 50% of the glomeruli were atrophic. Glomerular lipidosis was graded as severe if > 50% of the glomeruli showed accumulation of large foam cells in one or more lobules of the glomerular tuft; moderate when the accumulation of large foam cells in one or more lobules of a glomerular tuft affected 10% to 50% of the glomeruli. Tubular vacuolar degeneration was considered as severe if > 50% of tubular epithelial cells had variably sized clear vacuoles in the cytoplasm; moderate when the percentage of affected tubular epithelial cells was between 20% and 50%. Interstitial nephritis was defined as severe if tubules were replaced by inflammatory cells; moderate if inflammatory cells were present and only separate the tubules. Tubular atrophy was graded as severe if > 50% of tubular epithelial cells were atrophic (tubule with thickened and/or wrinkled basement membrane and simplification of tubular epithelial cells); moderate if the percentage of atrophic cells was between 20% and 50%. Tubular necrosis was considered as severe when > 50% of tubular epithelial cells was necrotic (tubular lumens containing sloughed, non-viable epithelial cells and/or cellular debris); moderate when the percentage of necrotic cells was between 10% and 50%. Fibrosis was considered as severe when > 50% of the specimen was affected; moderate when only 10% to 50% of the section was affected. Amyloidosis was considered as severe when a confluence of the amyloid deposits, or a global effacement of most glomeruli (> 50%) was evident; moderate when only small scattered deposits in multiple glomeruli were evident.

The overall score for one kidney was the mean of the scores assigned to the three sampled portions. The neoplastic samples were excluded from the study. All the histological samples were blindly analysed by two of the authors, FB and GM, with over 6 and over 3 years' experience in histopathology respectively. Differences in scores were resolved by consensus achieved through simultaneous viewing using a dual-headed microscope.

Table 1
Complete results of the Anova of renal ultrasonographic abnormalities for the degenerative score groups. Results of the post-hoc tests reporting the differences among individual degenerative score groups are also reported.

Ultrasonographic abnormality	F-value	p-value	Post-hoc
Cortico-medullary definition	6.532	< 0.001	0–2
Echogenicity of the cortex	17.678	< 0.001	0–1, 0–2, 1–2
Echogenicity of the medullary	8.289	< 0.001	0–2
Shape	9.612	< 0.001	0–2, 1–2
Cyst	2.120	0.126	–
Scars	7.764	< 0.001	0–2, 1–2
Mineralization	1.227	0.298	–
Pyelectasia	11.731	< 0.001	0–2, 1–2

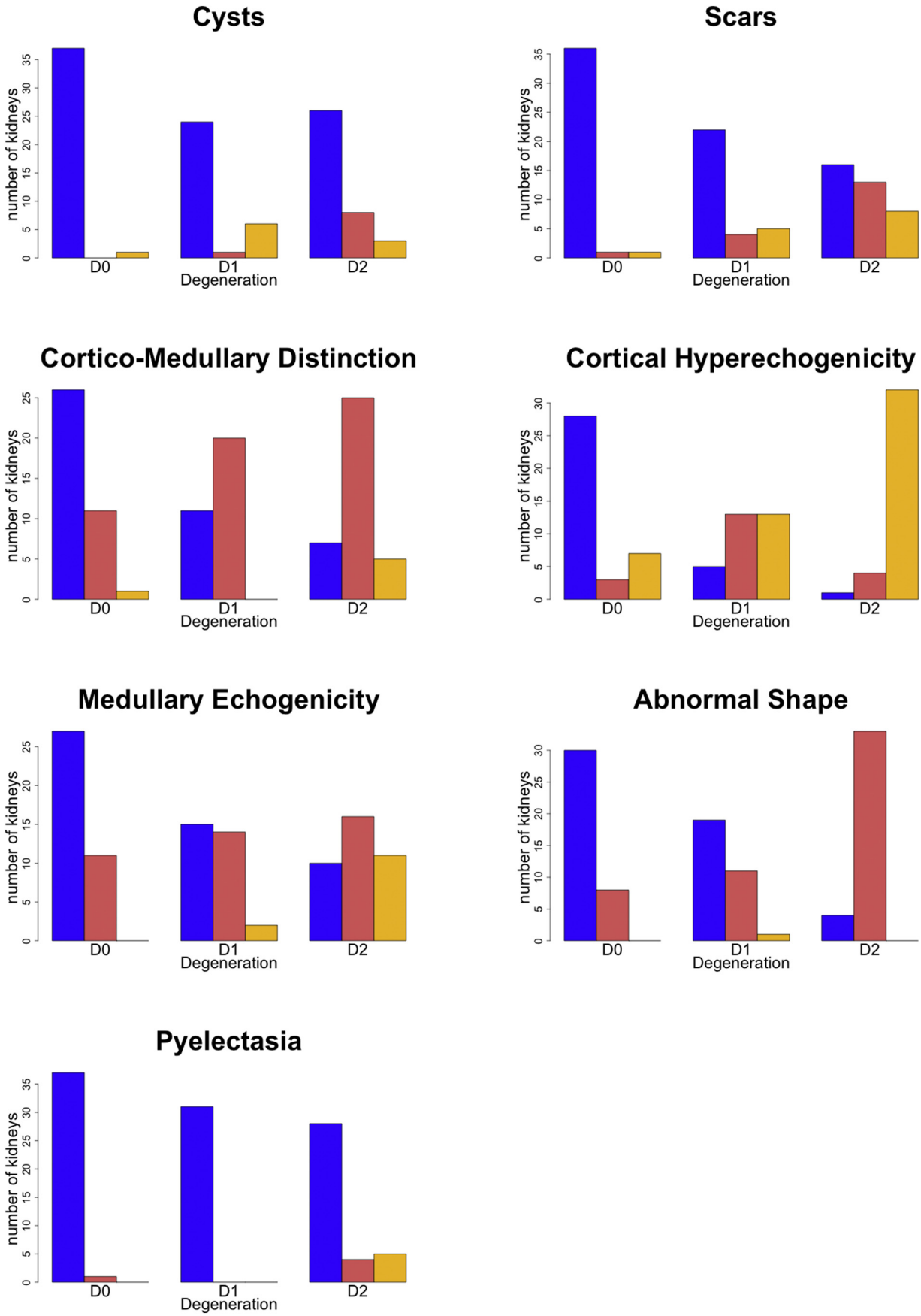

Fig. 1. Bar charts illustrating the number of kidneys showing each ultrasonographic abnormality classified by the degeneration score assigned by the pathologist.

Table 2
Complete results of the Anova of renal ultrasonographic abnormalities for the inflammatory score groups. Results of the post-hoc tests reporting the differences among individual inflammatory score groups are also reported.

Ultrasonographic abnormality	F-value	p-value	Post-hoc
Cortico-medullary definition	4.426	0.015	0–1
Echogenicity of the cortex	0.778	0.465	–
Echogenicity of the medullary	2.256	0.111	–
Shape	4.925	0.009	0–2, 1–2
Cyst	0.232	0.793	–
Scars	3.403	0.037	0–2
Mineralization	2.626	0.797	–
Pyelectasia	1.448	0.241	–

2.5. Statistical analysis

All the statistical analysis was performed using the R programing language R Core Team, 2013. R: a language and environment for statistical computing. R Foundation for Statistical Computing, Vienna, Austria, URL http://www.R-project.org/).The probability distribution of the variable RUS was tested. The correlation between each ultrasonographic abnormality, the RUS, and the degeneration and the inflammation scores was tested using a linear mixed model considering the patient as a random factor. Differences in the least square means were tested using an Anova test. Multiple comparison tests were performed with the Tukey-Kramer test. $P < .05$ was considered significant in all the statistical analysis.

3. Results

Fifty-five dogs were included in the study: 22 females and 33 males, weighing from 3 to 52 kg, mean age of 9.8 ± 4 years. Thirty-nine kidneys were classified with a degenerative score of 2, 32 with a degenerative score of 1, and 39 as showing no degeneration under histopathological examination. Twenty-two kidneys were classified with an inflammatory score of 2, and 28 with an inflammatory score of 1, whereas 60 kidneys showed no signs of inflammation under histopathological examination. Forty-four kidneys were classified in both the degenerative and inflammatory score groups, and 33 were classified as showing no degeneration and with no signs of inflammation. Lastly, six kidneys showed only inflammatory changes. Statistically significant differences in cortico-medullary definition, echogenicity of the renal cortex, echogenicity of the medulla, renal shape, scars and pyelectasia were evident between the degeneration score groups. No significant differences were evident for kidneys showing cysts or mineralizations. Complete results of the Anova and the post-hoc tests for each ultrasound abnormality in the degenerative score groups are reported in Table 1. In addition, bar charts illustrating the number of kidneys showing each ultrasound abnormality classified by the degeneration score assigned by the pathologists are reported in Fig. 1.

There was a significantly different distribution of cortico-medullary definition, renal shape and scars between inflammatory score groups, while all the remaining ultrasound abnormalities (echogenicity of the renal cortex, echogenicity of the medulla, cysts, mineralizations and pyelectasia) showed no significant differences among the inflammatory score groups. Complete results of the Anova and the post-hoc tests for each ultrasound abnormality in the inflammatory score groups are reported in Table 2. Bar charts illustrating the number of kidneys showing each US abnormality classified by the inflammatory score assigned by the pathologist are reported in Fig. 2. Since no patient had subcapsular fluid accumulation, we excluded the perirenal fluid parameter from the statistical analysis.

There were statistically significant differences in the RUS between the degenerative score groups ($F = 24.154$, p-value $< .001$), with a large effect estimate (1.6 RUS) of the random factor (patient). Post-hoc tests revealed significant differences between all groups. The least square means of the RUS of the different degenerative score groups are reported in Table 3.

There were no significant differences in the RUS between the inflammatory score groups ($F = 1.312$, p-value $= .264$). Post-hoc tests revealed no significant differences between groups. The least square means of the RUS of the different inflammatory score groups are reported in Table 4.

4. Discussion

The correlation between renal ultrasound and renal pathology is a controversial topic (Bragato et al., 2017). The results of this study suggest that renal degeneration should always be suspected if changes in the US appearance are evident, except for cystic or mineralized patterns. Indeed, as a result of this study, abnormalities in the echogenicity of the renal cortex ($F = 17.678$, $p < .001$), pyelectasia ($F = 11.731$, $p < .001$), renal shape ($F = 9.612$, $p < .001$), and echogenicity of the medulla ($F = 8.239$, $p < .001$) showed the largest differences among the degeneration score groups. Interestingly, similar US abnormalities (abnormal renal shape, cortical hyperechogenicity, medulla hyperechogenicity) were correlated to reduced renal function in the study by Mattei et al., 2019. It is the authors' opinion that, such results highlight the potential of ultrasound in the prediction of both the functionality and the histopathological status of the kidneys. It should be stated here, even if it goes beyond the aims of a study focusing on the canine species, that Lamb et al. (2017) found that small kidneys, hyperechoic renal cortex, loss of corticomedullary differentiation, renal calculi, enlarged kidneys, and dilated renal pelvis were statistically associated with decreased renal function in cats. Further studies, ideally evaluating ultrasound, renal function, and renal histopathology at the same time, could clarify the complex relationship between these three different aspects of renal pathology.

The least square means of the RUS of the degeneration-affected kidneys was significantly higher than that of kidneys showing no degeneration. These results highlight the moderate correlation between the amount and the severity of renal ultrasonographic abnormalities and the degree of renal degeneration. On the other hand, the least square means of the RUS of the kidneys showing no degeneration was 1.12, meaning that some ultrasonographic abnormalities could be present even if no degeneration is detectable by means of histopathology. It is the authors' opinion that this might, at least partially, be related to the subjective assessment of the ultrasonographic signs; it could be possible that some lesions might have been overlooked during the ultrasonographic examinations. On the other hand, also the methodology used for the histopathological sampling of the kidneys might have led to some subjectivity. Indeed, mild and focal degenerative changes might not have been identified by the pathologists and, therefore, not considered in classification of the samples.

Significant differences were evident only between individual US abnormalities (cortico-medullary definition, shape, scars) and renal inflammation, whereas no significant differences raised in the inflammation score groups when the ultrasonographic lesions were considered in an aggregate form (the RUS). It is the authors' belief that such results suggest that it is not possible to detect inflammatory changes of the kidneys by means of ultrasound alone. We should state at this point, however, that none of the dogs had ultrasonographic (perirenal or retroperitoneal fluid) or histopathological signs that are usually associated with acute kidney inflammation (Holloway and O'Brien, 2007).

In the previous studies by some of the authors (Banzato et al., 2017; Zotti et al., 2015), renal cortical echogenicity was measured quantitatively through a dedicated software whereas renal cortical echogenicity was assessed subjectively by two of the authors in this protocol. This difference is due to the fact that, for technical reasons, two different scanners were used to acquire the US images and, therefore, a reliable comparison between the quantitative values was not possible. Indeed,

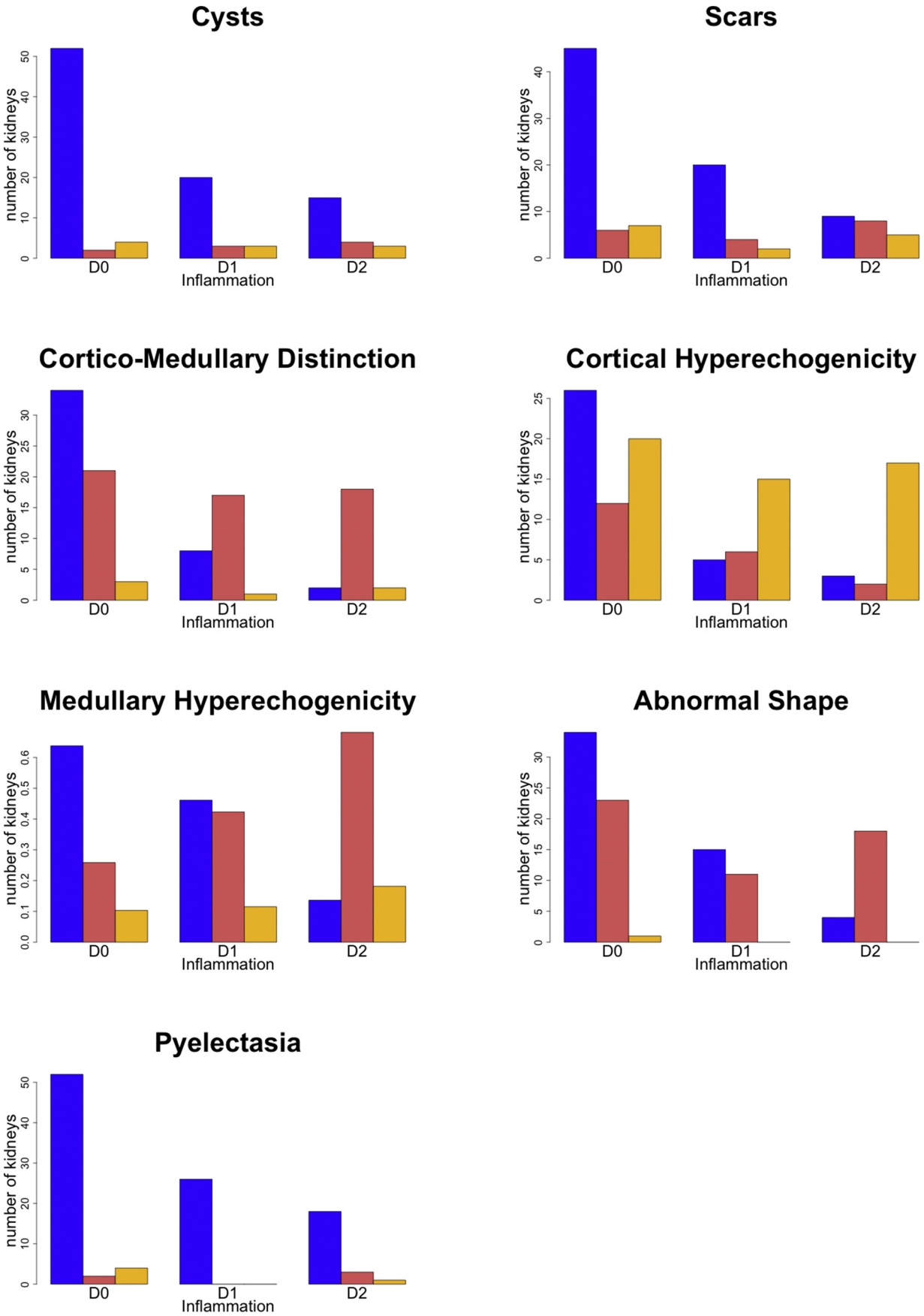

Fig. 2. Bar charts illustrating the number of kidneys showing each ultrasonographic abnormality classified by the inflammatory score assigned by the pathologist.

Table 3
Least square means of the RUS as classified by the degenerative score assigned by the pathologists.

Degenerative score	Least square mean	Standard error	95% Confidence interval
0	1.12	0.231	0.66–1.58
1	1.89	0.223	1.45–2.33
2	2.91	0.234	2.44–3.37

Table 4
Least square means of the RUS as classified by the inflammatory score assigned by the pathologists.

Degenerative score	Least square mean	Standard error	95% Confidence interval
0	1.81	0.239	1.33–2.28
1	2.06	0.269	1.53–2.60
2	2.28	0.298	1.68–2.87

the repeatability of quantitative analysis of the ultrasound images is limited by the different imaging protocols used by different US scanners (Manley and O'Neill, 2001). Both the ultrasonographic abnormalities and the degeneration and inflammation scores were decided after a consensus discussion between two experienced operators, thus limiting the bias deriving from inter-observer variability. Interestingly, the results obtained in this study regarding the relationships occurring between cortical renal echogenicity and the renal parenchymal histopathological status are similar to those obtained in a previous *in-vivo* study (Banzato et al., 2017). Other authors (Mattei et al., 2019), have used the echogenicity of the spleen to obtain comparable results as baseline for a subjective evaluation of renal cortical echogenicity. It is the authors' opinion that such a comparison is highly unreliable, primarily because this methodology assumes the spleen to be normal.

The ultrasound abnormalities included here are commonly evaluated and annotated during a routine clinical ultrasound procedure. Classification of the US abnormalities was partially adapted from similar papers published by Lamb et al., 2017, and Mattei et al., 2019. In addition to the ultrasonographic abnormalities, Mattei et al., 2019, also included several kidney measurements in the analysis (*e.g.*:kidney and medullary length, width and height, and aorta diameter). Kidney measurements were not included in the present study mainly because the ultrasound scans were performed in a clinical setting and aorta diameter was not routinely evaluated. Interestingly, Mattei et al., 2019, concluded that, although some statistically significant differences between the size of normal kidneys and kidneys with reduced glomerular filtration were evident, the significant overlap between these two groups largely limits the usefulness of these measurements in the dog.

A weakness of the present study is that renal biomarkers (serum creatinine and urea nitrogen levels) were available only for 33 of the dogs and, therefore, these were not included in the statistical analysis. In addition, the relationship between renal degeneration and renal serum creatinine levels in dogs remains unclear (Hokamp and Nabity, 2016), and other, more specific biomarkers such as the glomerular filtration rate or symmetric dimethylarginine are required for a thorough evaluation of the kidney function. On the other hand, the ultrasound appearance of all the organs is mainly related to their histological characteristics and only marginally to their function. Therefore, the correlation between renal ultrasonographic abnormalities and renal function is, at the least, equivalent to the correlation between renal function and renal pathology.

5. Conclusions

The descriptive parameter (RUS) proposed in this study showed significant differences between all the degeneration score groups, meaning that the number and severity of the ultrasonographic abnormalities are correlated with the severity of kidney degeneration. On the other hand, inflammation showed little influence on the ultrasonographic appearance of the kidneys.

Funding

The present paper is part of a project funded by a research grant from the Department of Animal Medicine, Production and Health – MAPS, University of Padua, Italy: SID- Zotti 2018 (€ 32,000; Application of deep-learning algorithms in pet animal diagnostic imaging).

Authors' contributions

TB: conceived the study, performed the ultrasonographic examinations, drafted and revised the manuscript.

FB: performed the histological examinations, drafted and revised the manuscript.

AZ: conceived the study, performed the ultrasonographic examinations, drafted and revised the manuscript.

GM: collected the kidneys and performed the histological examinations.

Declaration of Competing Interest

The authors declare that they have no competing interests.

References

Aresu, L., Benali, S., Ferro, S., Vittone, V., Gallo, E., Brovida, C., Castagnaro, M., 2013. Light and electron microscopic analysis of consecutive renal biopsy specimens from Leishmania-seropositive dogs. Vet. Pathol. 50, 753–760. https://doi.org/10.1177/0300985812459336.

Banzato, T., Bonsembiante, F., Aresu, L., Zotti, A., 2017. Relationship of diagnostic accuracy of renal cortical echogenicity with renal histopathology in dogs and cats, a quantitative study. BMC Vet. Res. 13, 24. https://doi.org/10.1186/s12917-016-0941-z.

Bragato, N., Borges, N.C., Fioravanti, M.C.S., 2017. B-mode and doppler ultrasound of chronic kidney disease in dogs and cats. Vet. Res. Commun. 41, 307–315. https://doi.org/10.1007/s11259-017-9694-9.

Cianciolo, R.E., Mohr, F.C., Aresu, L., Brown, C.A., James, C., Jansen, J.H., Spangler, W.L., van der Lugt, J.J., Kass, P.H., Brovida, C., Cowgill, L.D., Heiene, R., Polzin, D.J., Syme, H., Vaden, S.L., van Dongen, A.M., Lees, G.E., 2016. World small animal veterinary association renal pathology initiative: classification of glomerular diseases in dogs. Vet. Pathol. 53, 113–135. https://doi.org/10.1177/0300985815579996.

Espada, Y., Novellas, R., Ruiz de Gopegui, R., 2006. Renal ultrasound in dogs and cats. Vet. Res. Commun. 30, 133–137. https://doi.org/10.1007/s11259-006-0026-8.

Hart, D.V., Winter, M.D., Conway, J., Berry, C.R., 2013. Ultrasound appearance of the outer medulla in dogs without renal dysfunction. Vet. Radiol. Ultrasound 54https://doi.org/10.1111/vru.12069. n/a-n/a.

Hokamp, J.A., Nabity, M.B., 2016. Renal biomarkers in domestic species. Vet. Clin. Pathol. 45, 28–56. https://doi.org/10.1111/vcp.12333.

Holloway, A., O'brien, R., 2007. Perirenal effusion in dogs and cats with acute renal failure. Vet. Radiol. Ultrasound 48, 574–579. https://doi.org/10.1111/j.1740-8261.2007.00300.x.

Ivancic, M., Mai, W., 2008. Qualitative and quantitative comparison of renal vs. hepatic ultrasonographic intensity in healthy dogs. Vet. Radiol. Ultrasound 49, 368–373. https://doi.org/10.1111/j.1740-8261.2008.00383.x.

Lamb, C.R., Dirrig, H., Cortellini, S., 2017. Comparison of ultrasonographic findings in cats with and without azotaemia. J. Feline Med. Surg. 1098612X1773665. J. Feline Med. Surg. https://doi.org/10.1177/1098612X17736657. 1098612X1773665.

Lee, S., Hong, S., Kim, H., Oh, D., Kim, S., Choen, S., Choi, M., Yoon, J., 2017. Ultrasonographic evaluation of renal cortex and outer medulla thickness in dogs with chronic kidney disease. J. Vet. Clin. 34, 208–212. https://doi.org/10.17555/jvc.2017.06.34.3.208.

Manley, J.A., O'Neill, W.C., 2001. How echogenic is echogenic? Quantitative acoustics of the renal cortex. Am. J. Kidney Dis. 37, 706–711. https://doi.org/10.1016/S0272-6386(01)80118-9.

Mattei, C., Pelander, L., Hansson, K., Uhlhorn, M., Olsson, U., Häggström, J., Ljungvall, I., Ley, C.J., 2019. Renal ultrasonographic abnormalities are associated with low glomerular filtration rate calculated by scintigraphy in dogs. Vet. Radiol. Ultrasound. https://doi.org/10.1111/vru.12755. m, vru.12755.

Moghazi, S., Jones, E., Schroepple, J., Arya, K., McClellan, W., Hennigar, R.A., O'Neill, W.C., 2005. Correlation of renal histopathology with sonographic findings. Kidney

Int. 67, 1515–1520. https://doi.org/10.1111/j.1523-1755.2005.00230.x.
Morrow, K.L., Salman, M.D., Lappin, M.R., Wrigley, R., 1996. Comparison of the resistive index to clinical parameters in dogs with renal disease. Vet. Radiol. Ultrasound 37, 193–199. https://doi.org/10.1111/j.1740-8261.1996.tb01220.x.
O'Neill, W.C., 2000. Sonographic evaluation of renal failure. Am. J. Kidney Dis. 35, 1021–1038. https://doi.org/10.1016/S0272-6386(00)70036-9.
Wang, J.-H., Hung, C.-H., Kuo, F.-Y., Eng, H.-L., Chen, C.-H., Lee, C.-M., Lu, S.-N., Hu, T.-H., 2013. Ultrasonographic quantification of hepatic–renal echogenicity difference in hepatic steatosis diagnosis. Dig. Dis. Sci. 58, 2993–3000. https://doi.org/10.1007/s10620-013-2769-8.
Zotti, A., Banzato, T., Gelain, M.E., Centelleghe, C., Vaccaro, C., Aresu, L., 2015. Correlation of renal histopathology with renal echogenicity in dogs and cats: an ex-vivo quantitative study. BMC Vet. Res. 11, 99. https://doi.org/10.1186/s12917-015-0415-8.